RSC Advances

PAPER

View Article Online
View Journal | View Issue

Cite this: *RSC Adv.*, 2022, **12**, 18004

Functional drug carriers formed by RGD-modified β-CD-HPG for the delivery of docetaxel for targeted inhibition of nasopharyngeal carcinoma cells

Lingling Xu,*[ab] Chuan Zhou,*[ac] Fan Wang,*[d] Huiqin Liu,[ac] Guangyuan Dong,[ac] Siyi Zhang†[ab] and Tao Liu †[ab]

In this study, a drug delivery system was prepared by grafting the targeting molecule arginine-glycine-aspartic acid (RGD) onto hyperbranched polyglycerol (HPG)-modified β-cyclodextrin (β-CD-HPG) for the targeted inhibition of nasopharyngeal carcinoma (NPC) cells. The obtained β-CD-HPG-RGD with a relatively small size and low surface charge delivered docetaxel (Doc) effectively and displayed a targeting effect to human NPC HNE-1 cells, as confirmed by confocal laser scanning microscopy and flow cytometry. The *in vitro* drug release analysis exhibited the controlled drug release kinetics of the β-CD-HPG-RGD/Doc nanomedicine. β-CD-HPG-RGD/Doc effectively inhibited the proliferation of HNE-1 cells and promoted apoptosis. Moreover, its biocompatibility *in vitro* and *in vivo* was assessed. The results indicate that the β-CD-HPG-RGD/Doc nanomedicine has potential application in NPC targeting therapy.

Received 11th April 2022
Accepted 26th May 2022

DOI: 10.1039/d2ra02301f

rsc.li/rsc-advances

Introduction

Nasopharyngeal carcinoma (NPC) is endemic in southern China, with a high incidence in five provinces, including Guangdong, Hainan, Guangxi, Hunan, and Fujian, especially in people living in the Pearl River Delta and West Pearl River Valley in Guangdong. NPC ranks 11th among the malignant tumors in China, with an incidence of 1.9/100 000 person-years in females and 2.8/100 000 person-years in males.[1] Accordingly, docetaxel (Doc) has been demonstrated to be suitable for the treatment of advanced NPC patients with metastasis and its therapeutic effect is clear.[2] Doc is a cytotoxic drug that selectively kills tumor cells without producing toxic effects on normal cells. However, similar to most clinical chemotherapy drugs, Doc has low solubility in an aqueous environment, which leads to its low bioavailability.[3,4] Thus, over the past several years, a variety of nanoplatforms has been explored to improve the targeting specificity and solubility of Doc.[5,6] Nanomedicine can significantly improve the treatment efficiency and reduce adverse reactions.[7]

Cyclodextrins (CDs) are cyclic oligomers consisting of at least six D-(+)-glucopyranose units connected by α-(1–4) bonds.[8] CDs have been used as a supramolecular linker due to the abundant guest molecules that can interact with their cavity to form supramolecular inclusion complexes.[9] There are three types of CDs, *i.e.*, α-, β-, and γ-CD, consisting of six, seven, and eight glucose units, respectively.[10] Among them, β-CD possesses several advantages including availability, biocompatibility, and low toxicity.[11] Furthermore, β-CD can form inclusion complexes with many types of hydrophobic chemotherapeutic drugs due to the molecular structure of its lipophilic internal cavities and hydrophilic external surfaces.[10] However, reports show that the simple introduction of β-CD only improves the solubility of hydrophobic drugs to a limited extent.[12] Therefore, increasing the solubility of β-CD to get stable, biocompatible drug carriers is highly desirable.

Hyperbranched polyglycerol (HPG) has hyperbranched polyol-like structures, featuring a random distribution of functional groups throughout its globular structure.[13] Recently, many researchers have devoted much attention to HPGs due to their excellent biocompatibility, high water solubility, low toxicity, one-step production process, and good thermal stability.[14] Moreover, the large number of hydroxyls in the straight and terminal positions of HPG increases its water solubility.[15] Therefore, HPGs are now considered promising drug delivery carriers, especially for hydrophobic drugs.

[a]*Department of Otolaryngology-Head and Neck Surgery, Guangdong Provincial People's Hospital, Guangdong Academy of Medical Sciences, Guangzhou, Guangdong 510080, China. E-mail: szhang555@hotmail.com; taoliu18@126.com*

[b]*The Second School of Clinical Medicine, Southern Medical University, Guangzhou, Guangdong 510515, China*

[c]*Shantou University Medical College, Shantou, 515063, PR China*

[d]*Key Laboratory of Biomaterials of Guangdong Higher Education Institutes, Department of Biomedical Engineering, Jinan University, Guangzhou, 510632, China*

† Siyi Zhang and Tao Liu are co-corresponding authors.

Doc is a cytotoxic drug that selectively kills tumor cells without producing adverse effects on normal cells. However, tumor-targeting ligands can guide anti-tumor drug-conjugated NPs to reach specific tumor tissue and achieve better therapeutic effects, while reducing drug toxicity. Hu and co-workers reported a method for the synthesis of cationic folic acid-loaded micelles, which could incorporate active drugs in tumor cells.[16] To improve the drug targeting toward cancer cells, antibodies or peptides with tumor cell-specific binding sites can be modified on the surface of carriers.[17,18] The high-affinity interaction between the RGD tripeptide (arginine-glycine-aspartic acid) and $\alpha_v\beta_3$ integrin has aroused great interest in cancer targeting therapies.[19,20] This is because $\alpha_v\beta_3$ integrin is generally overexpressed on the surface of cancer cells,[21,22] and consequently can serve as a vast potential target for cancer-targeting therapeutics. Some researchers grafted RGD peptides on the surface of drug delivery carriers, which could remarkably enhance the drug accumulation in carcinoma cells to improve therapeutic outcomes and reduce severe side effects.[23–25]

In the present study, a drug delivery system was prepared by grafting the targeting molecule RGD onto HPG-modified β-cyclodextrin (β-CD-HPG) for the targeted inhibition of NPC cells. An antitumor drug, Doc, was encapsulated in β-CD-HPG-RGD to form β-CD-HPG-RGD/Doc nanomedicine. The structure and physicochemical properties of this drug delivery carrier were characterized. Furthermore, the targeted cellular uptake and cytotoxic effect were also studied using NPC HNE-1 cells.

Experimental

Materials and measurements

β-cyclodextrin (β-CD), glycidol, potassium hydride, 18-crown-6,4-dimethylamino pyridine (DMAP), dimethylformamide (DMF), triethylamine (Et_3N), succinic anhydride, 1-ethyl-3-(3-dimethylaminopropyl)carbodiimide hydrochloride (EDC), *N*-hydroxy succinimide (NHS), RGD peptide and docetaxel (Doc) were purchased from Aladdin Chemistry Co., Ltd (Shanghai, China). All chemicals were of analytical grade and used as received. β-CD was used after drying under vacuum at 40 °C for 48 h. Glycidol was stored in a refrigerator at −8 °C and purified by vacuum distillation before the reaction. Potassium hydride was dispersed in mineral oil and kept in the dark. 18-Crown-6 was stored in a desiccator.

The ^{1}H NMR spectra of the nanoparticles were measured on a Varian Unity-Plus 400 MHz spectrometer in D_2O. The Fourier transform infrared (FTIR) spectra of the nanoparticles were recorded using an FTIR spectrometer (SHIMADZU IRAffinity-1, Japan). A dynamic light scattering (DLS) particle size analyzer (Zetasizer Nano laser nanometer particle sizer, Malvern) at 173° scattering was used to measure the average diameter of the samples at 25 °C. The zeta potential of the samples was measured using a zeta potential meter (Zetasizer Nano laser nanometer particle sizer, Malvern) at 25 °C.

Synthesis of β-CD-HPG-RGD

β-CD-HPG was prepared *via* the anionic ring-opening multi-branching polymerization (ROMBP) method.[26] Firstly, 0.99 g of 18-crown-6 and 0.6 g of 6-EDA-β-CD were dispersed in 25 mL of dry dimethylformamide (DMF). After they completely dissolved, potassium hydride (KH, 0.168 g) was slowly added to the mixture at the reaction temperature of 90 °C and stirred for 2 h under magnetic stirring. Then, 10.86 mL of glycidol was added dropwise to the reaction after the temperature was lowered to 80 °C, and the mixture was stirred for 24 h under anhydrous and anaerobic conditions. After the reaction was complete, a small amount of ultrapure water was added and the reaction was cooled to room temperature. Subsequently, the resultant mixture was dialyzed and purified with a dialysis bag (MWCO = 1000, USA) for 3 days, and finally the product β-CD-HPG was obtained after freeze-drying.

Purified β-CD-HPG (200 mg) and succinic anhydride (100 mg) were dissolved in 10 mL of DMF. Next, a mixture of 4-dimethylamino pyridine (DMAP, 120 mg) and triethylamine (Et_3N, 1 mL) was dissolved in 2 mL of DMF and the mixture was added to the above-mentioned solution and stirred for 24 h at 70 °C under nitrogen. Under this condition, the hydroxy groups of β-CD-HPG reacted with succinic anhydride. Finally, the obtained β-CD-HPG-COOH was dialyzed (MWCO = 1000, USA) against distilled water for 3 days to remove the excess reagents before the solution was freeze-dried.

About 6 mL of an aqueous solution of β-CD-HPG-COOH (10 mg mL^{-1}) was mixed with 600 μL of freshly prepared aqueous solution of 1-ethyl-3-(3-dimethylaminopropyl)-carbodiimide hydrochloride (EDC, 20 mg mL^{-1}) and 600 μL of aqueous solution of *N*-hydroxy succinimide (NHS, 25 mg mL^{-1}). The pH of the solution was adjusted to 7.4 by adding PBS buffer and stirring for 30 min. Next, 1.5 mL of an aqueous solution of (RGDfK) peptide (2 mg mL^{-1}) was added and stirred overnight. Finally, the resultant β-CD-HPG-RGD was dialyzed (MWCO = 2000) against distilled water for 3 days to remove the remaining reagents and free peptide.

Evaluation of the drug loading capacity

For the loading of the hydrophobic Doc, initially, we dissolved β-CD-HPG-RGD in distilled water at a concentration of 10 mg mL^{-1}, and then Doc in acetone at a concentration of 3 mg mL^{-1} was added dropwise within 1 h to the above-mixed solution in an ice bath. The mixture was magnetically stirred for 24 h at room temperature in the dark. Next, the resulting mixture was placed in a dialysis bag (MWCO = 1000) for 1 h to remove the acetone. Then, the dialysate was passed through a syringe filter (0.45 μm pore size) to remove the non-encapsulated drug. Finally, β-CD-HPG-RGD/Doc was obtained after lyophilization.

The drug loading capacity (LC) was determined *via* high performance liquid chromatography (HPLC; UV detector, model 5200 A Coulochem II, Agilent 1200, USA). β-CD-HPG-RGD/Doc was dissolved in the mobile phase, and then HPLC was used to analyze the loading amount. The measurement was conducted with a mobile phase consisting of acetonitrile, methanol, and deionized water (40/35/25) at the flow rate of 1.0 mL min^{-1} and the detection wavelength was 230 nm. The LC was calculated as follows:

$$\text{LC\%} = \text{weight of Doc in NPs/weight of NPs} \times 100\%$$

In vitro drug release

In vitro release profiles of Doc from β-CD-HPG-RGD/Doc were measured in PBS containing 1% (w/v) Tween 80. The samples (5 mL) were introduced into a dialysis tube (MWCO = 1000) and incubated in 20 mL of buffer at 37 °C with horizontal shaking. At predetermined intervals (0.5 h, 1 h, 2 h, 4 h, 8 h, 10 h, 12 h, 24 h, 48 h, 72 h, and 96 h), 5 mL of the release medium was extracted and the same volume of fresh buffer was added. In our work, the Doc release profile was fitted to the Korsmeyer–Peppas equation $M_t/M_\infty = kt^n$ ($M_t/M_\infty \leq 60\%$).[27,28] The concentration of Doc was measured *via* HPLC (UV detector, model 5200 A Coulochem II, Agilent 1200, USA) and its standard curve was calculated as follows:

$$Y = 55675X \ (R^2 = 0.999)$$

where X is the concentration of Doc and Y is the peak area. The drug release assay of all the samples was performed in triplicate and the error bars in the plot are the standard deviation.

Cellular uptake study

The cellular uptake of the β-CD-HPG-RGD-Cy5 and β-CD-HPG-Cy5 NPs was evaluated *via* confocal laser scanning microscopy (CLSM; Leica, Germany) and flow cytometry (BD Biosciences, USA). HNE-1 cells were seeded in 24-well plates with a density of 5×10^4 cells per well. After incubation for 24 h, fresh RPMI-1640 medium containing β-CD-HPG-RGD-Cy5 or β-CD-HPG-Cy5 (10 μg mL^{-1}) was added for 0.5 h, 1 h, 2 h, 4 h, and 8 h respectively. After trypsinizing and washing twice with PBS, the HNE-1 cells were resuspended in 200 μL of PBS, and the cellular internalization efficiency was evaluated by flow cytometry. The statistical analysis was carried out using Flow Jo 7.6.1. The cell internalization rate was calculated using the following formula: cell internalization rate = fluorescence of the experimental group/fluorescence of the control group × 100%.

Besides, the cellular uptake of β-CD-HPG-RGD-Cy5 and β-CD-HPG-Cy5 NPs was observed using CLSM. HNE-1 cells were first incubated with β-CD-HPG-RGD-Cy5 or β-CD-HPG-Cy5 NPs for 1 h, respectively. Then, the medium was removed and the cells were fixed with 4% paraformaldehyde (Merck) at room temperature for 15 min, followed by washing with PBS twice. The cell membrane was labeled by incubating cells with DIO (Thermo Fisher Scientific) for 15 min at 37 °C. Cell nuclei were stained by incubation with DAPI (Thermo Fisher Scientific) for 10 min at 37. Finally, the intracellular localization of β-CD-HPG-RGD-Cy5 was visualized under a laser scanning confocal microscope.

Cellular toxicity

The suppression effects of free Doc, β-CD-HPG-RGD, and β-CD-HPG-RGD/DOC were evaluated using HNE-1 cells. The cell line was seeded in a 96-well plate (about 1×10^4 per well) with 100 μL RPMI-1640 medium in a humidified atmosphere of 5% CO_2 at 37 °C for 24 h. Then, the medium was replaced with 100 μL RPMI-1640 medium containing free DOC, β-CD-HPG-RGD or β-CD-HPG-RGD/Doc with different concentrations (1 μg mL^{-1}, 0.5 μg mL^{-1}, 0.1 μg mL^{-1}, 0.05 μg mL^{-1}, 0.01 μg mL^{-1}, and 0.001 μg mL^{-1}), and RPMI-1640 medium was set as the negative control group. After 24 h incubation (37 °C, 5% CO_2), the culture medium was removed and the HNE-1 cells were washed with PBS twice. Then, 100 μL RPMI-1640 medium containing 10 μL CCK-8 per well was added. The plates were placed in 5% CO_2 at 37 °C for 2 h before measurement. The absorbance at 450 nm was measured by using a microplate reader. Cell viability was calculated according to the following formula:

$$\text{Cell viability}(\%) = (A - B)/(C - B) \times 100\%$$

where A, B, and C represent the absorbance values measured in the microplate reader by the sample solution, background, and fresh medium aperture control group, respectively.

Apoptosis assay

The cell apoptosis assay was analyzed by Annexin V-PE/7-AAD stained flow cytometry (BD Biosciences, USA). Briefly, HNE-1 cells were seeded in a 24-well culture plate (about 5×10^4 cells per well) and incubated for 24 h in RPMI-1640 medium. Then, the medium was replaced with 2 mL RPMI-1640 medium containing free Doc, β-CD-HPG-RGD, or β-CD-HPG-RGD/Doc at the Doc concentration of 1 μg mL^{-1}. After the treatments, as described above, the HNE-1 cells were trypsinized and washed with PBS twice. Thereafter, the cells were resuspended with 200 μL of 1× binding buffer. Then, 5 μL Annexin V-PE and 5 μL 7-AAD were added to each sample, mixed gently, and incubated for 15 min in the dark at room temperature. Finally, the stained cells were recorded by flow cytometry within 1 h and analyzed using the Flow Jo 7.6.1 software.

Biocompatibility *in vitro*

The biocompatibility of β-CD and β-CD-HPG-RGD to 3T3 cells *in vitro* was characterized using the CCK-8 assay. Firstly, 3T3 cells were seeded in 96-well culture plates (about 1×10^4 cells per well) and incubated for 24 h in RPMI-1640 medium containing 10% FBS and 1% penicillin-streptomycin. Then, the cells were incubated with 100 μL RPMI-1640 medium containing β-CD or β-CD-HPG-RGD at different concentrations (1 mg mL^{-1}, 0.5 mg mL^{-1}, 0.1 mg mL^{-1}, 0.05 mg mL^{-1}, 0.01 mg mL^{-1}, 0.005 mg mL^{-1}, and 0.001 mg mL^{-1}) at 37 °C for 24 h, and RPMI-1640 medium without sample was set as the negative control group. After removing the medium, the cells were washed with phosphate buffer solution (PBS; 0.1 M, pH 7.4) twice and incubated in 100 μL RPMI-1640 medium containing 10 μL CCK-8 (Cell Counting Kit-8) for another 2 h. The absorbance at 450 nm was measured by using a microplate reader. Cell viability was calculated according to the following formula:

$$\text{Cell viability}(\%) = (A - B)/(C - B) \times 100\%$$

where A, B, and C represent the absorbance values measured in the microplate reader by the sample solution, background, and a fresh medium aperture control group, respectively.

In vivo toxicity

Female 4 weeks-old Balb/*c* nude mice were purchased from Hunan SJA Laboratory Animal Co., Ltd (Hunan, China). The animals were housed in specific pathogen-free (SPF) conditions at 20–26 °C and 50–70% relative humidity with standard animal food and water ad libitum. The nude mice were randomly divided into two groups ($n = 5$). Subsequently, the mice were injected through their tail vein with 200 μL β-CD-HPG-RGD (5 μg g^{-1}) and 200 μL PBS, respectively. After 7 days, the animals were sacrificed and their major organs (liver, kidney, spleen, brain, heart and lung) harvested and washed with PBS. After fixing in 4% formaldehyde, histological examination was carried out.

Ethics statement

The animal experiments were performed according to the Animal Ethics Committee of Guangdong Provincial People's Hospital (No. GDREC2019830A). All animals received humane care in compliance with good animal practice according to the animal ethic procedures and guidelines of China.

Statistical analysis

All quantitative experiments were carried out three times. The data are expressed as mean ± standard deviation (SD). Significant differences between two groups were detected using one-way analysis of variance (ANOVA). $P < 0.05$ was considered statistically significant.

Results and discussion

Synthetic strategy and material characterization

β-CD-HPG-RGD was synthesized according to the synthesis route shown in Fig. 1. The synthetic strategy to obtain β-CD-HPG involves ring-opening multi-branching polymerization at the hydroxyl group-terminated surface of β-CD. This procedure results in the grafting of HPG at the surface of β-CD and the formation of water-soluble β-CD-HPG. Next, the terminal hydroxyl groups of β-CD-HPG are reacted with succinic anhydride, which generates carboxylic acid-terminated β-CD (β-CD-HPG-COOH). Finally, RGD peptide functional β-CD-HPG (β-CD-HPG-RGD) was prepared by grafting RGD with the carboxy groups on HPG through amidation. The chemical structure of β-CD-HPG-RGD was confirmed by solution-phase 1H. As shown in Fig. 2, the NMR signal of the H2–H6 protons on the cyclodextrin nucleus and the proton signal peaks (3.2–4.5 ppm) on the methylene and methylene groups of HPG overlap for β-CD-HPG-RGD. However, the characteristic signal peak of cyclodextrin H1 in β-CD-HPG is still distinct (4.9–5.1 ppm), where it only changed from the sharp H1 signal peak of pure cyclodextrin to a covered broad peak, indicating that the polymer product contained cyclodextrin units and had the properties of polymer macromolecules. In addition, the aromatic Ha signal on RGD

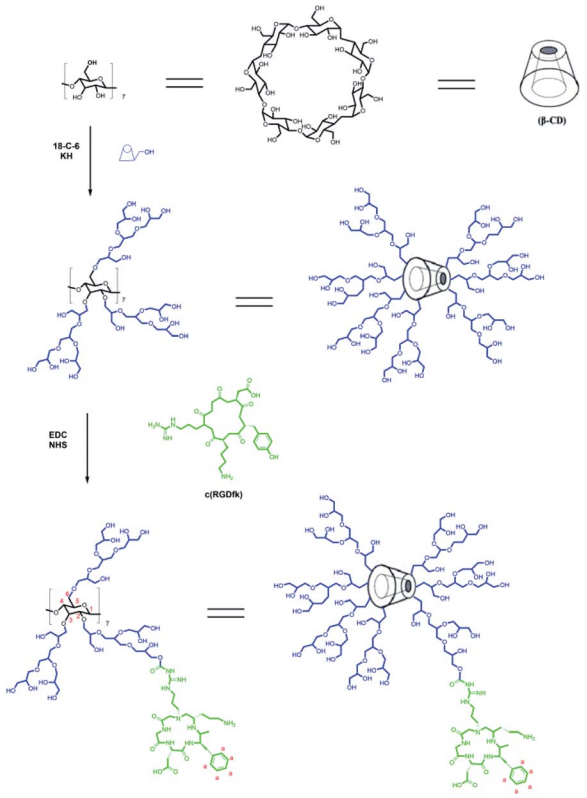

Fig. 1 Synthetic route for β-CD-HPG-RGD.

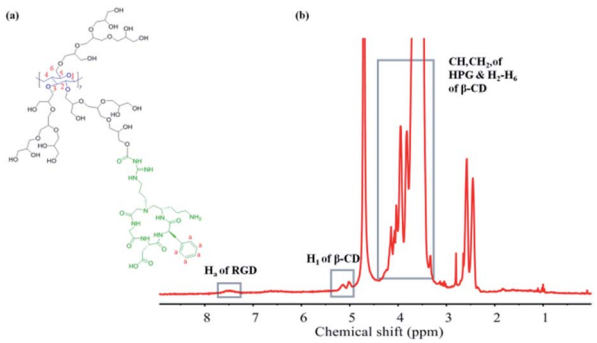

Fig. 2 (a) Chemical structure of β-CD-HPG-RGD. (b) ^{1}H NMR spectrum of β-CD-HPG-RGD in D_2O.

showed a significant peak at 7.1–7.7 ppm. These results show the successful synthesis of β-CD-HPG-RGD.

Alternatively, the grafting of RGD onto HPG was confirmed by FTIR spectroscopy (Fig. 3). The spectrum of HPG showed an intense band at 1458 cm^{-1}, which was assigned to the C=O stretching bond. In addition, the FTIR spectrum of RGD showed an intense band at 1650 cm^{-1}, corresponding to the amido bond. The FTIR spectrum of HPG-RGD displayed both the signature of HPG for stretching vibration of C=O and RGD for that of the amido bond at 1458 cm^{-1} and 1650 cm^{-1}, respectively.

The surface charge of β-CD-HPG, RGD, and β-CD-HPG-RGD was evaluated by zeta potential measurement (Fig. 4).

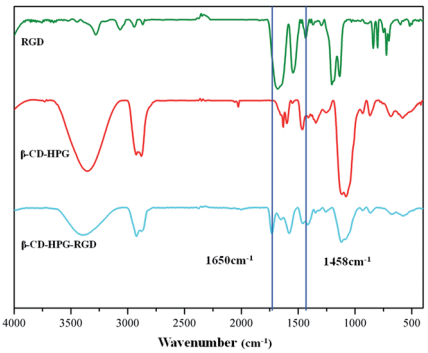

Fig. 3 FTIR spectra of RGD, β-CD-HPG and β-CD-HPG-RGD.

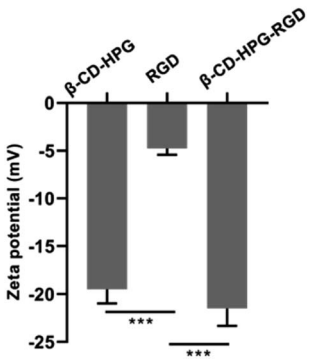

Fig. 4 Zeta potential of β-CD-HPG, RGD, and β-CD-HPG-RGD. ***P < 0.001.

Comparing the three types of NPs, the zeta potential of β-CD-HPG-RGD was slightly more negative than that of β-CD-HPG and RGD. The reason for this phenomenon could be that the conjugation with the RGD peptides consumed a fraction of the carboxylate groups.

The size of β-CD-HPG, RGD, and β-CD-HPG-RGD was studied using a dynamic light scattering (DLS) particle size analyzer. The results (Fig. 5) show that the size of β-CD-HPG-RGD increased after grafting RGD, suggesting the efficient grafting of RGD on the surface of β-CD-HPG. By contrast, the relatively smaller size increase of β-CD-HPG-RGD is due to the modification with small molecules and inconspicuous particle aggregation.

We proposed the possible self-assembly process of β-CD-HPG-RGD in water. Driven by the strong hydrophobic interactions of their hydrophobic groups, the β-CD-HPG-RGD molecules spontaneously assemble into aggregates. Simultaneously, intermolecular interactions through hydrogen bonds may also cause the aggregation of β-CD-HPG-RGD. However, the hydrogen bond interactions between the aggregates and the water molecules and the surface charge of β-CD-HPG-RGD, which can act as a repelling force, may prevent further aggregation. Aggregates have been widely observed in self-assembled hyperbranched polymers in the literature.[29,30]

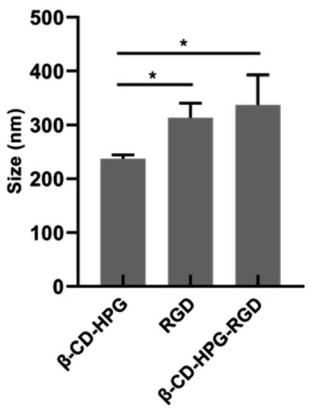

Fig. 5 DLS results of β-CD-HPG, RGD, and β-CD-HPG-RGD. *P < 0.05.

Drug loading capacity and release behavior

In this work, the drug loading capacity and drug behavior of Doc in the β-CD-HPG-RGD composites were examined to evaluate their potential for the delivery of hydrophobic drugs. We demonstrated that the loading capability of Doc on β-CD-HPG-RGD is 8.47 wt%. This high drug LC can be attributed to the extra drug loading in the HPG branches. Fig. 6 shows the cumulative Doc release profile from β-CD-HPG-RGD. In the β-CD-HPG-RGD/Doc release curve, about 40% of Doc was released in the first 8 h. The initial burst release of Doc may be due to the Doc molecules located on the NP surfaces. This was followed by a slow continuous release phase, which can be attributed to the hydrophobic interactions between Doc and the hydrophobic interior of the NPs.[30] The release kinetics of Doc from β-CD-HPG-RGD/Doc depends on many factors, including particle size, polymer degradation rate, and molecular weight of the hydrophobic and hydrophilic segments.[31] β-CD-based drug delivery carriers could efficiently control the drug release rate.[11] Thus, considering the high drug LC and the controlled release behavior of β-CD-HPG-RGD, it is a promising hydrophobic drug delivery system.

Cellular uptake

We used flow cytometry and CLSM to confirm the cellular uptake behavior of β-CD-HPG-RGD against $\alpha_v\beta_3$ receptor-positive HNE-1 cells. The HNE-1 cells were incubated with

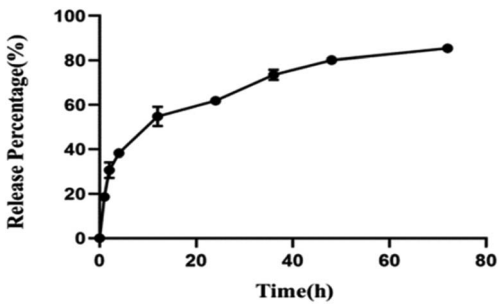

Fig. 6 Cumulative Doc release profile from β-CD-HPG-RGD/Doc.

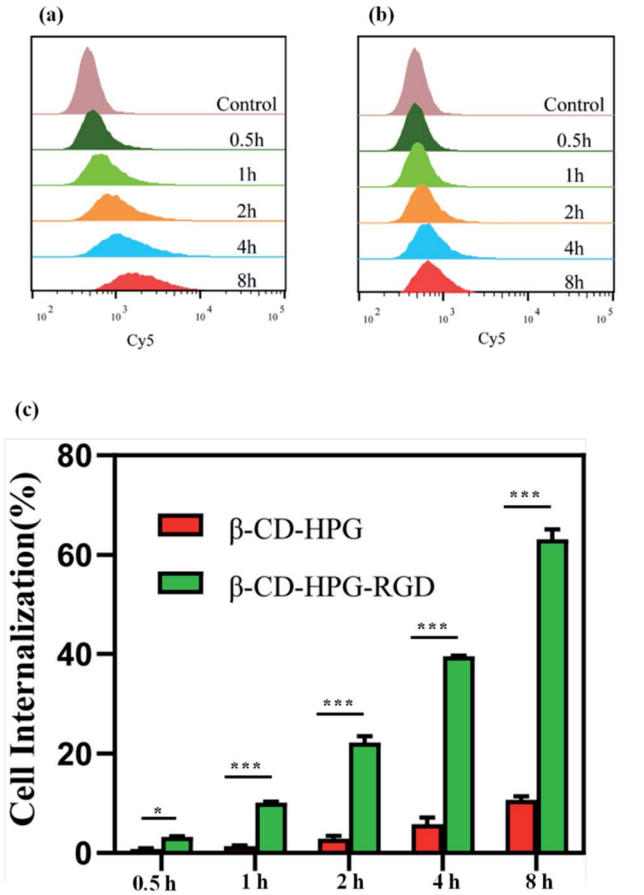

Fig. 7 Flow cytometry relative fluorescence intensity of β-CD-HPG-Cy5 (a) and β-CD-HPG-RGD-Cy5 (b). (c) Cell internalization assay of HNE-1 cells. *P < 0.05 and ***P < 0.001.

Cy5-labeled-β-CD-HPG or Cy5-labeled-CD-HPG-RGD for 0.5 h, 1 h, 2 h, 4 h, and 8 h, respectively, and the cells without any treatment were used as the control group. Remarkably, the flow cytometry data demonstrated that much more β-CD-HPG-RGD was taken up by the HNE-1 cells than β-CD-HPG. Meantime, the uptake of β-CD-HPG-RGD by cells appeared to be time-dependent (Fig. 7c).

Fig. 8 shows the CLSM images of the cells incubated with β-CD-HPG-Cy5 or β-CD-HPG-RGD-Cy5 for 1 h. The data clearly shows that β-CD-HPG-RGD was internalized in the cells more effectively than β-CD-HPG. This is consistent with the flow cytometry data. The higher cellular uptake of β-CD-HPG-RGD can be ascribed to receptor-mediated endocytosis,[32,33] depending on the $\alpha_v\beta_3$ receptors, which are generally overexpressed on the surface of tumor cells and tumor vascular endothelial cells.[34] The flow cytometry data and the CLSM images indicate that β-CD-HPG-RGD exhibited desirable characteristics as a drug delivery carrier for targeted NPC therapy.

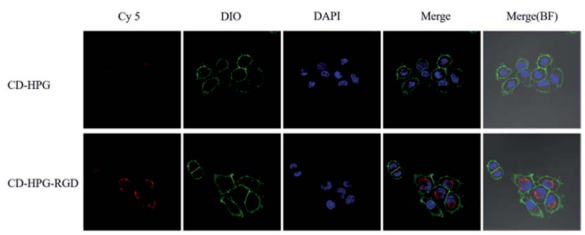

Fig. 8 CLSM images of HNE-1 cells incubated with β-CD-HPG-Cy5 and β-CD-HPG-RGD-Cy5 for 1 h.

In vitro cytotoxicity

To evaluate the potential of this drug delivery system in NPC therapy, we tested its tumor cell proliferation inhibition effect on HNE-1 cells *via* the CCK-8 method. The effects of free Doc, β-CD-HPG-RGD and β-CD-HPG-RGD/Doc on the viability of HNE-1 cells 24 h post-treatment are shown in Fig. 9. When the concentration of Doc ranged from 0.001–1 μg mL^{-1}, β-CD-HPG-RGD showed low cytotoxicity, while free Doc and β-CD-HPG-RGD/Doc exhibited concentration-dependent inhibition of the proliferation of HNE-1 cells. Notably, the proliferation inhibition effect on HNE-1 cells by the RGD-mediated NPs was not more significant than free Doc, which may be owing to the incomplete release of Doc from β-CD-HPG-RGD/Doc.

Alternatively, as a small molecule, Doc can promptly enter cells through passive diffusion without driven energy.[35] This result illustrates that β-CD-HPG-RGD is an outstanding Doc carrier, which not only had good hydrophobic drug delivery ability but also maintained the efficacy of the free drug, which presented an excellent therapeutic effect.

In vitro apoptosis assay

We used the apoptosis assay to further validate the effects of this drug delivery system on NPC therapy by performing Annexin V-PE and 7-AAD staining. Annexin V-PE and 7-AAD can distinguish early or late apoptosis and living cells or necrotic cells, respectively.[33] As shown in Fig. 10, after incubation with blank β-CD-HPG-RGD for 24 h, the cells showed inconspicuous apoptosis compared to the control group. By contrast, the free Doc and β-CD-HPG-RGD/Doc displayed drastic apoptotic rates. These results are consistent with the CCK-8 assay results. We assumed that the free Doc diffused into the cells rapidly and

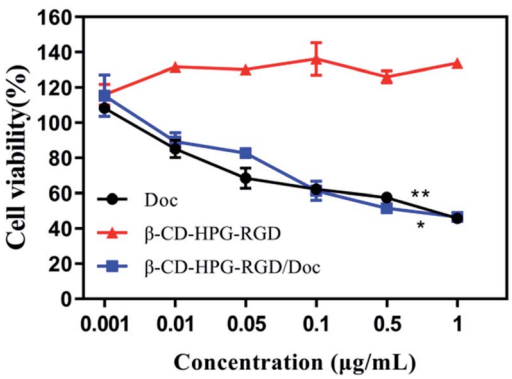

Fig. 9 CCK-8 assay for HNE-1 cells after 24 h incubation with various samples. *P < 0.05 and **P < 0.01 *vs.* the β-CD-HPG-RGD groups.

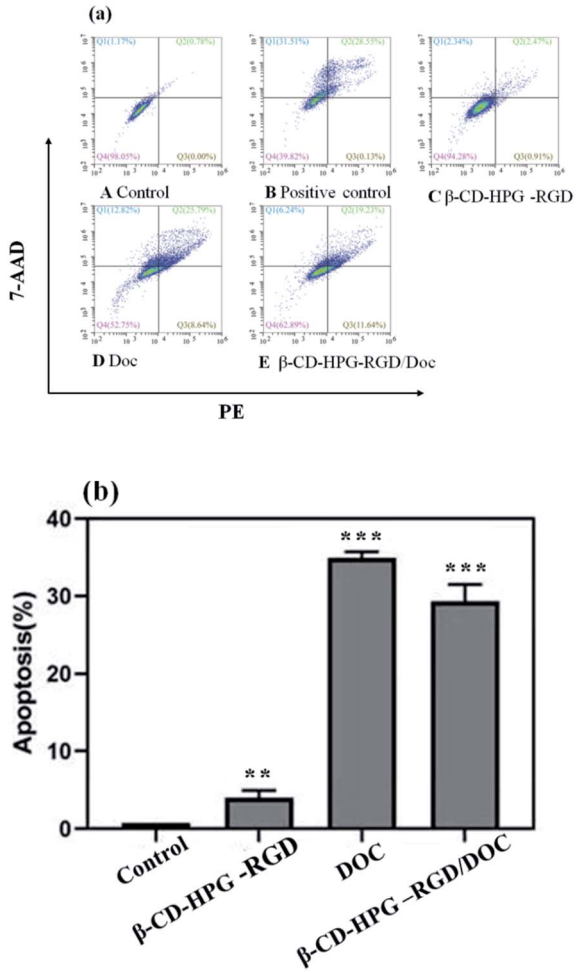

Fig. 10 (a) Apoptosis analysis of HNE-1 cells after 24 h incubation with the various samples. (b) Apoptosis cell proportion. $^{**}P < 0.01$ and $^{***}P < 0.001$ *vs.* the control groups.

completely after 24 h. However, in the case of β-CD-HPG-RGD/Doc, after completing receptor-mediated endocytosis, the NPs may have to overcome some other obstacles, such as endosomal escape. Therefore, β-CD-HPG-RGD is a promising effective, and safe carrier for hydrophobic drugs, which has potential application in NPC treatment.

Biocompatibility *in vitro*

As a drug carrier, the biocompatibility of β-CD or β-CD-HPG-RGD is a primary factor to be evaluated. The standard fibroblast cell line 3T3 was employed for the cytotoxicity determination of β-CD and β-CD-HPG-RGD. As shown in Fig. 11, neither β-CD nor β-CD-HPG-RGD in the concentration range of 0.001–1 mg mL^{-1} showed any significant toxicity to 3T3 cells after 24 h treatment, suggesting that this biocompatible composite is suitable for drug delivery applications. The low toxicity of β-CD-HPG-RGD can be expected because of the biocompatibility of β-CD and HPG.[11,14] This result indicates the cytotoxicity of the drug-loaded composite came from the Doc released from the composite. Accordingly, we concluded that β-CD-HPG-RGD with

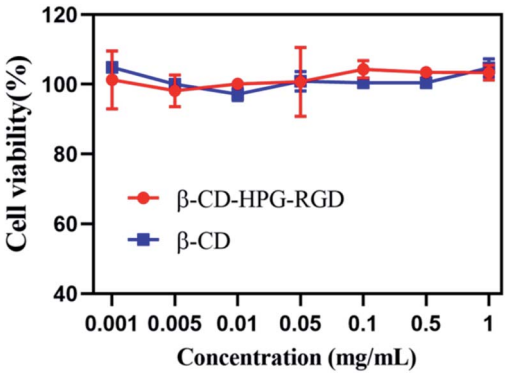

Fig. 11 Cell viability of β-CD and β-CD-HPG-RGD for 3T3 cells after 24 h incubation.

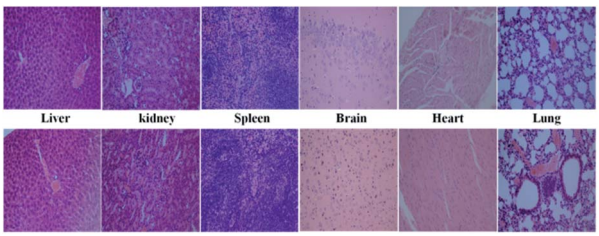

Fig. 12 Representative HE stain images of organ histology for β-CD-HPG-RGD (top row) and PBS control (bottom row).

outstanding biocompatibility may be considered as a potential targeting drug delivery system.

In vivo toxicity assay

An *in vivo* toxicity assay was also performed through histological analysis to prove the safety of β-CD-HPG-RGD. As shown in Fig. 12, there was no obvious difference in histology between the two groups. The *in vivo* toxicity of NPs is affected by their chemical structure, metabolism process, size and surface groups.[36] As we elaborated above, both β-CD and HPG exhibited excellent biocompatibility according to previous reports. Meanwhile, the hyperbranched molecular structure and the degradation ability of HPG could also contribute to the increased compatibility of the β-CD-HPG-RGD NPs.[37] Therefore, these compatible NPs are suitable for drug delivery.

Conclusion

In this work, an architecture composed of β-CD-HPG and RGD was successfully synthesized and characterized. Doc, as a hydrophobic drug, was effectively encapsulated in β-CD-HPG-RGD and its sustained release behavior was confirmed. *In vitro*, the antitumor assay showed that β-CD-HPG-RGD/Doc effectively inhibited the proliferation of HNE-1 cells. According to the CLSM and flow cytometry analyses, β-CD-HPG-RGD displayed a significant targeting function toward HNE-1 cells compared to β-CD-HPG, which may be attributed to RGD receptor-mediated endocytosis. Moreover, the empty NPs, β-CD-HPG-RGD, showed

low cytotoxicity despite their high concentration *in vitro* and *in vivo*. Therefore, β-CD-HPG-RGD NPs possess promising applications for NPC-targeting drug delivery.

Conflicts of interest

There are no conflicts to declare.

Acknowledgements

This work was supported by the Natural Science Foundation of Guangdong Province (2019A1515011678), the Science and Technology Program of Guangzhou City (202002030065), the talent introduction fund of Guangdong Provincial People's Hospital [Y012018142], and the matching scientific research fund for Guangdong Provincial outstanding young medical talent by Guangdong Provincial People's Hospital [KJ012019454].

References

1 S. Cao, M. Simons and C. Qian, *Chin. J. Cancer*, 2011, **30**, 114–119.
2 S. Ferrati, E. Nicolov, S. Bansal, S. Hosali, M. Landis and A. Grattoni, *Curr. Drug Targets*, 2015, **16**, 1645–1649.
3 Z. Hami, M. Amini, M. Ghazi-Khansari, S. Rezayat and K. Gilani, *Colloids Surf., B*, 2014, **116**, 309–317.
4 J. Ngeow, W. Lim, S. Leong, M. Ang, C. Toh, F. Gao, B. Chowbay and E. Tan, *Ann. Oncol.*, 2011, **22**, 718–722.
5 H. Maeda, H. Nakamura and J. Fang, *Adv. Drug Delivery Rev.*, 2013, **65**, 71–79.
6 V. Shargh, H. Hondermarck and M. Liang, *Nanomedicine*, 2016, **11**, 63–79.
7 K. Javed, M. Ahmad, S. Ali, M. Butt, M. Nafees, A. Butt, M. Nadeem and A. Shahid, *Medicine*, 2015, **94**, e617.
8 T. Loftsson and M. Brewster, *J. Pharm. Sci.*, 1996, **85**, 1017–1025.
9 Y. Xin, H. Wang, B.-w. Liu and J.-y. Yuan, *Chin. J. Polym. Sci.*, 2014, **33**, 36–48.
10 K. Cal and K. Centkowska, *Eur. J. Pharm. Biopharm.*, 2008, **68**, 467–478.
11 B. Gidwani and A. Vyas, *Colloids Surf., B*, 2014, **114**, 130–137.
12 U. Gupta, H. Agashe, A. Asthana and N. Jain, *Biomacromolecules*, 2006, **7**, 649–658.
13 D. Wilms, S. Stiriba and H. Frey, *Acc. Chem. Res.*, 2010, **43**, 129–141.
14 M. Rahman, M. Alrobaian, W. Almalki, M. Mahnashi, B. Alyami, A. Alqarni, Y. Alqahtani, K. Alharbi, S. Alghamdi, S. Panda, A. Fransis, A. Hafeez and S. Beg, *Drug discovery today*, 2021, **26**, 1006–1017.
15 M. Gosecki, M. Gadzinowski, M. Gosecka, T. Basinska and S. Slomkowski, *Polymers*, 2016, **8**, 1–25.
16 Y. Hu, L. Gan, Q.-x. Li, H. Tao, L. Ye, A.-y. Zhang and Z.-g. Feng, *Chin. J. Polym. Sci.*, 2014, **32**, 1714–1723.
17 P. Jiao, M. Otto, Q. Geng, C. Li, F. Li, E. Butch, S. Snyder, H. Zhou and B. Yan, *J. Mater. Chem. B*, 2016, **4**, 513–520.
18 D. Tesauro, A. Accardo, C. Diaferia, V. Milano, J. Guillon, L. Ronga and F. Rossi, *Molecules*, 2019, **24**, 351–378.
19 C. Boswell, P. Eck, C. Regino, M. Bernardo, K. Wong, D. Milenic, P. Choyke and M. Brechbiel, *Mol. Pharmaceutics*, 2008, **5**, 527–539.
20 J. Morlieras, S. Dufort, L. Sancey, C. Truillet, A. Mignot, F. Rossetti, M. Dentamaro, S. Laurent, L. Vander Elst, R. Muller, R. Antoine, P. Dugourd, S. Roux, P. Perriat, F. Lux, J. Coll and O. Tillement, *Bioconjugate Chem.*, 2013, **24**, 1584–1597.
21 W. Cai and X. Chen, *Anti-Cancer Agents Med. Chem.*, 2006, **6**, 407–428.
22 L. Lacaria, J. Lange, W. Goldmann, F. Rico and J. Alonso, *Biochem. Biophys. Res. Commun.*, 2020, **525**, 836–840.
23 M. Amin, A. Badiee and M. Jaafari, *Int. J. Pharm.*, 2013, **458**, 324–333.
24 L. Battistini, P. Burreddu, A. Sartori, D. Arosio, L. Manzoni, L. Paduano, G. D'Errico, R. Sala, L. Reia, S. Bonomini, G. Rassu and F. Zanardi, *Mol. Pharmaceutics*, 2014, **11**, 2280–2293.
25 W. Chen, Y. Zou, Z. Zhong and R. Haag, *Small*, 2017, **13**, 1601997.
26 W. Tao, Y. Liu, B. Jiang, S. Yu, W. Huang, Y. Zhou and D. Yan, *J. Am. Chem. Soc.*, 2012, **134**, 762–764.
27 M. Sajjad, M. Khan, S. Naveed, S. Ijaz, O. Qureshi, S. Raza, G. Shahnaz and M. Sohail, *AAPS PharmSciTech*, 2019, **20**, 81.
28 H. Vardhan, P. Mittal, S. Adena and B. Mishra, *Eur. J. Pharm. Sci.*, 2017, **99**, 85–94.
29 H. Cheng, S. Wang, J. Yang, Y. Zhou and D. Yan, *J. Colloid Interface Sci.*, 2009, **337**, 278–284.
30 X. Zhang, X. Zhang, Z. Wu, X. Gao, C. Cheng, Z. Wang and C. Li, *Acta Biomater.*, 2011, **7**, 585–592.
31 S. Kim, J. Ha and Y. Lee, *J. Controlled Release*, 2000, **65**, 345–358.
32 L. Bareford and P. Swaan, *Adv. Drug Delivery Rev.*, 2007, **59**, 748–758.
33 J. Gao, C. Zhang, X. Fu, Q. Yi, F. Tian, Q. Ning and X. Luo, *PLoS One*, 2013, **8**, e63084.
34 O. Schnell, B. Krebs, E. Wagner, A. Romagna, A. Beer, S. Grau, N. Thon, C. Goetz, H. Kretzschmar, J. Tonn and R. Goldbrunner, *Brain Pathol.*, 2008, **18**, 378–386.
35 Y. Cao, Y. Gu, H. Ma, J. Bai, L. Liu, P. Zhao and H. He, *Int. J. Biol. Macromol.*, 2010, **46**, 245–249.
36 S. Li, C. Li, S. Jin, J. Liu, X. Xue, A. Eltahan, J. Sun, J. Tan, J. Dong and X. Liang, *Biomaterials*, 2017, **144**, 119–129.
37 T. Liu, X. Wu, S. Chen, P. Wu, H. Han, H. Zhang, J. Li, G. Li and S. Zhang, *Drug Delivery*, 2019, **26**, 1280–1291.